JACS
JOURNAL OF THE AMERICAN CHEMICAL SOCIETY

Communication

pubs.acs.org/JACS

Imaging Single-Chain Nanoparticle Folding via High-Resolution Mass Spectrometry

Jan Steinkoenig,[§,⊥] Hannah Rothfuss,[§,⊥] Andrea Lauer,[§,⊥] Bryan T. Tuten,[§,⊥] and Christopher Barner-Kowollik*[,§,⊥,‡]

[§]Preparative Macromolecular Chemistry, Institut für Technische Chemie und Polymerchemie, Karlsruhe Institute of Technology (KIT), Engesserstraße 18, 76128 Karlsruhe, Germany

[⊥]Institut für Biologische Grenzflächen, Karlsruhe Institute of Technology (KIT), Hermann-von-Helmholtz-Platz 1, 76344 Eggenstein-Leopoldshafen, Germany

[‡]School of Chemistry, Physics and Mechanical Engineering, Queensland University of Technology (QUT), 2 George Street, Brisbane, QLD 4000, Australia

Supporting Information

ABSTRACT: Herein, we introduce the first approach to map single-chain nanoparticle (SCNP) folding via high-resolution electrospray ionization mass spectrometry (ESI MS) coupled with size exclusion chromatography. For the first time, the successful collapse of polymeric chains into SCNPs is imaged by characteristic mass changes, providing detailed mechanistic information regarding the folding mechanism. As SCNP system we employed methyl methacrylate (MMA) statistically copolymerized with glycidyl methacrylate (GMA), resulting in p(MMA-*stat*-GMA), subsequently collapsed by using $B(C_6F_5)_3$ as catalyst. Both the precursor polymer and the SCNPs can be well ionized via ESI MS, and the strong covalent cross-links are stable during ionization. Our high-resolution mass spectrometric approach can unambiguously differentiate between two mechanistic modes of chain collapse for every chain constituting the SCNP sample.

Precisely folded single-chain polymer nanoparticles (SCNPs) have emerged as a major research area in the field of macromolecular architectures.[1] SCNPs generated through various motifs, such as Diels–Alder cycloadditions,[2] metal ligation,[3] hydrogen bonding,[1c,4] a variety of click and modular ligation chemistries,[5] and several reversible folding chemistries,[6] have found interesting applications in drug delivery,[7] imaging,[8] nano-containers, and catalysis.[9] Beyond the standard techniques utilized for characterizing these SCNPs (nuclear magnetic resonance (NMR) spectroscopy, infrared (IR) spectroscopy, size exclusion chromatography (SEC), dynamic light scattering (DLS), and diffusion-ordered NMR spectroscopy (DOSY)), more advanced techniques such as triple-detection SEC,[10] atomic force microscopy,[8] tunneling electron microscopy,[10] small-angle X-ray scattering,[11] and small-angle neutron scattering[11] have proven to be powerful tools in the morphological characterization of SCNPs. However, a shortcoming of these methods lies in the fact that they are not capable of imaging single chains and the individual chemical transformations they undergo. Herein, we introduce an advanced high-resolution electrospray ionization mass spectrometry (ESI MS) protocol for SCNP imaging. ESI MS is a powerful characterization tool employed for the structural elucidation of homo- and copolymers,[12] polyelectrolytes,[13] and various reaction pathways,[14] keeping the structural integrity of the chains intact based on the soft ionization process.[15] The structural elucidation can be further underpinned by employing collision-induced dissociation (CID) techniques such as higher-energy collision dissociation (HCD).

Scheme 1. Preparation of Poly(MMA-*stat*-GMA) (1) (M_n = 13 100 g·mol^{-1}, $Đ$ = 1.26) under RAFT Conditions (Bulk, 80 °C, 1 h) and Single-Chain Collapse Using $B(C_6F_5)_3$ as Catalyst for Intrachain ROP (a.t., 72 h)

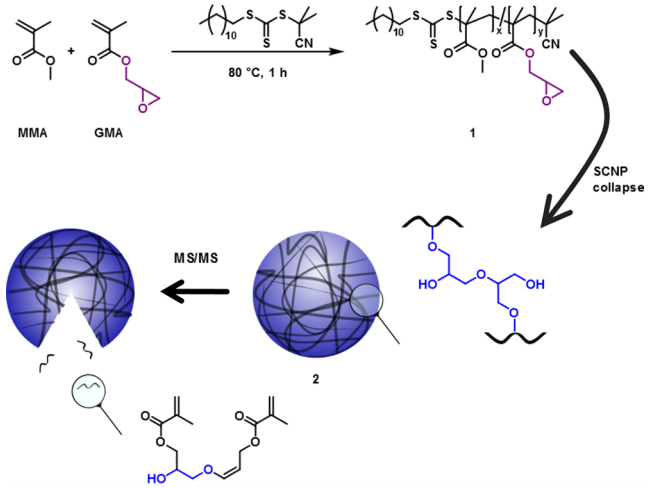

Taking inspiration from the work of Pomposo and co-workers,[16] a statistical copolymerization of methyl methacrylate (MMA) and glycidyl methacrylate (GMA) gave precursor polymer p(MMA-*stat*-GMA) (**1**), benefiting from the reversible addition–fragmentation chain transfer (RAFT) process, affording excellent end group fidelity. Subsequently, a Lewis acid catalyst, $B(C_6F_5)_3$,[17] initiates an intrachain cationic ring-opening polymerization (ROP),[18] collapsing the linear chain **1** into a nanoparticle, **2** (Scheme 1).[16]

Received: October 19, 2016
Published: December 14, 2016

DOI: 10.1021/jacs.6b10952
J. Am. Chem. Soc. 2017, 139, 51–54

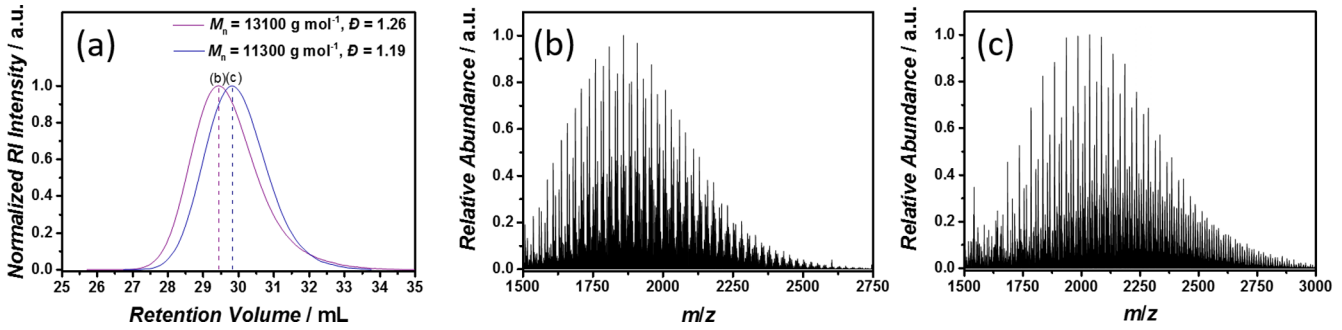

Figure 1. (a) SEC traces of p(MMA-*stat*-GMA) (**1**, purple line) and SCNP (**2**, blue line), illustrating the decrease of hydrodynamic radius. (b) SEC-ESI Orbitrap spectrum of **1** from m/z 1500 to 2750, depicting the single oligomer profiles of the double-charged copolymer species. (c) SEC-ESI Orbitrap spectrum of **2** from m/z 1500 to 3000, depicting the single oligomer profiles of the double-charged collapsed species.

We decided to utilize a methacrylate-type system for imaging SCNPs via mass spectrometry for three reasons: (i) pMMA—due to its complexation to Na^+—ionizes excellently; (ii) the ethylene glycol motifs resulting from the intrachain cross-linking event do not negatively affect the ionization;[19] and (iii) the intrachain ROP of glycidyl moieties allows for the elucidation of two possible collapse avenues, via a bimolecular coupling (i.e., a single glycidyl unit finds another glycidyl unit and reacts only once, terminating in a single ether bridge) or via propagation (i.e., one glycidyl unit ring-opens to find another glycidyl unit, which then ring-opens again to find another glycidyl unit, and so on). The solubility of precursor **1** and SCNP **2** allows for the characterization using SEC coupled with high-resolution ESI MS (SEC-ESI MS). As we reported previously,[20] the single oligomer profiles obtained by SEC-ESI MS are useful to assess the retention volume dependence of the single-, double-, or triple-charged species of the polymer. In the present study, we focused on the double-charged oligomer profiles (rather than the additionally observed single-, triple-, and quadruple-charged oligomer profiles) covering a broad mass range and thus high molar masses of p(MMA-*stat*-GMA) (**1**) and the SCNP **2**. More precisely, we performed the following experiments and mapped the resulting polymers: (i) direct addition of the catalyst $B(C_6F_5)_3$; (ii) slow addition of the catalyst with a syringe pump at a flow rate of 1 mL·h^{-1}; (iii) GMA feed ratios of 15% and 10% (with direct addition of the catalyst); (iv) multi-dimensional SEC-ESI MS^2 experiments to evidence the folding; and (v) aqueous quenching of all GMA units for a study in negative mode. To date, the limitation of the method is dictated by the ionization ability of the polymers (e.g., polar macromolecules), the accessible mass range (e.g., for Orbitrap <6000 m/z), and good solubility in THF (for SEC coupling).

Direct addition of the catalyst $B(C_6F_5)_3$ results in a reduced hydrodynamic radius of the polymer, as evidenced by the shift in the SEC trace to higher retention volume (Figure 1a). Comparison of the obtained mass spectra (Figure 1b,c) clearly illustrates that a chemical modification took place (see Figure S4 for a zoomed-in comparison). Due to statistics of the cross-linking event, we did not expect to find such a clear spectrum as illustrated in Figure 1c (for the zoomed-in spectrum, refer to Figure S9). Although the ion abundancy slightly decreased, SCNP **2** ionizes representatively and allows the clear assignment of species according to specific mechanisms (see below). A reduced ion abundance might be explained as follows: the catalyst $B(C_6F_5)_3$—considered as a strong Lewis acid—forms strong complexes with oxygen,[16] and thus the catalyst is coordinated to each initially ring-opened epoxide. During the aqueous workup, a Lewis acid exchange with a proton takes place. Therefore, each epoxide, which was ring-opened by the catalyst, carries a proton instead of the catalyst and—as proposed—is positively charged before injection into the ESI source. As a consequence, SCNPs containing many cross-links might become highly charged and cannot be analyzed sufficiently due to an unfavorable mass-to-charge ratio (leading to overlapping isotopic patterns and low abundant species as part of the background noise). Moreover, we observed a (cross) ionization between Na^+ (stemming from an external source) and a proton, or entirely by protons. To result in 100% sodium-ionized SCNPs, Na^+ stemming from an external source (added as 100 μmol of sodium iodide as doping agent) would have to diffuse into the SCNP during the spray process and the following ionization mechanism,[21] thereby replacing the protons. We assume that this process does not occur, as we did not observe any species being ionized entirely by Na^+.

SEC-ESI MS measurements performed in negative mode pointed to hypothetically positively charged SCNP **2**. As observed in negative mode, the SCNPs cannot be ionized negatively (neither by complexation to iodide nor by deprotonation events). We further established that the mass spectrometric mapping of a system based on aqueously quenched GMA can be realized in negative mode, thereby observing species ionized by virtue of complexation to iodide (see Figure S6). Thus, we believe that the SCNPs form a specific geometry, which hinders external ionization agents (as Na^+ or iodide) to exchange already existing charges (as a proton stemming from the Lewis acid exchange).

Therefore, direct addition of $B(C_6F_5)_3$ results in a mass spectrum (Figure 2a) where the species can be assigned to proton or proton/Na^+ ionized structures (Figure 2b). Each single peak contains up to four individual SCNP species. The presence of different SCNP species within each peak pattern was evidenced by the fusion of the individual contributing simulated isotopic patterns of each SCNP folding product (refer to Figures S10–S14). For instance, a species at m/z 2236 (labeled with ■) was assigned to a SCNP where two glycidyl moieties reacted with each other (m/z 2236.6506 (exp), 2236.6436 (theor)).

How many MMA units separate the ethylene glycol bridge formed during the SCNP collapse? Or, referring to Figure 2b, what is x if the sum of all MMA units is $x + y = 38$? We performed multi-dimensional SEC-ESI MS^2 experiments on the peak at m/z 2236, collecting all fragments after the tandem experiment (Figure S17) to find a species which would give the number of MMA units in one loop. However, even the lowest employed HCD energy already resulted in small-molecule fragments, albeit confirming the presence of the proposed ethylene glycol moiety (Table S3). Although we cannot identify the number of MMA

DOI: 10.1021/jacs.6b10952
J. Am. Chem. Soc. 2017, 139, 51–54

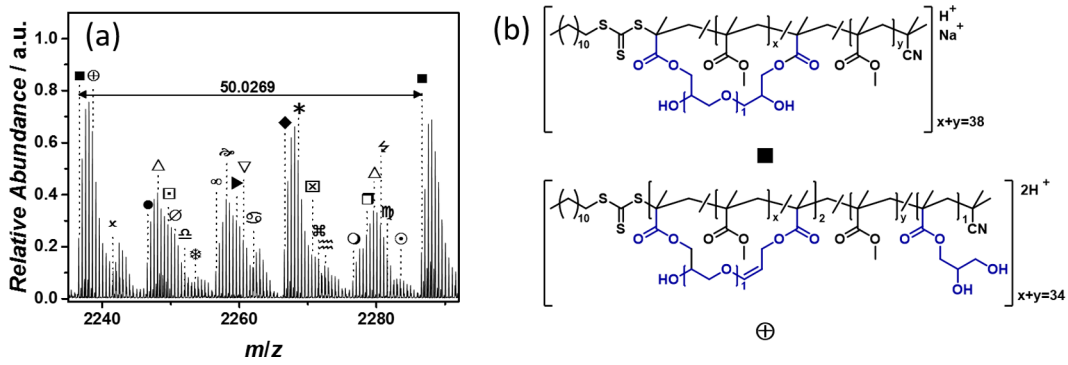

Figure 2. Direct addition of catalyst to produce SCNP **2**. (a) Zoomed-in SEC-ESI Orbitrap spectrum (positive mode) between m/z 2235 and 2292, obtained by summing up all species between 14.42 and 15.92 mL retention volume. Labeled are the most abundant species and the repeating unit of pMMA (m/z 50.0269 (exp), 50.0257 (theor)). (b) Structural assignment of the peak at m/z 2238 (see Figure S10 for the isotopic simulation). The structures have an estimated ratio of ■:⊕ = 5:1. For all structures and their assignments, refer to Table S2.

units separating the cross-links, we can clearly differentiate the folding mechanism.

In the following, we will discuss the two overarching mechanistic scenarios under which the folding can proceed based on the data shown in Figure 2. The data were obtained by having all reaction components—including the catalyst—from the beginning in the reaction mixture. Subsequently, we will discuss the results obtained by catalyst addition over a certain period of time. The mechanistic scenarios are (i) bimolecular coupling and (ii) propagation. First, the bimolecular coupling reaction involves only two GMA units (Figure 3a), and we assume

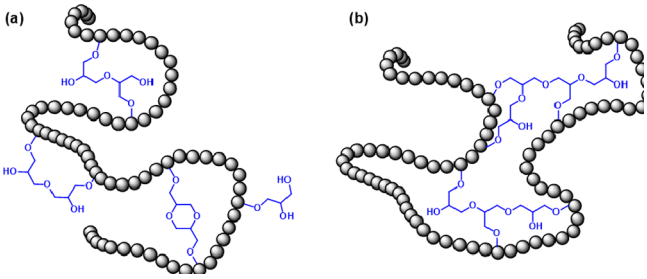

Figure 3. Schematic illustrations of (a) bimolecular coupling of two glycidyl moieties in different possible motifs and (b) propagation during cationic ROP with three and four glycidyl units involved.

the bimolecular coupling as entropically favored.[22] In a scenario of a linear chain undergoing a folding process, the global chain flexibility is maximized (thereby maximizing entropy), despite the sterically strained and inflexible loop being formed as a result of the bimolecular coupling. If a second bimolecular coupling event occurs, the chain loses again an amount of entropy formed by the sterically strained loop at a different position of the chain. Thus, a bimolecular coupling event always creates a SCNP with maximized entropy by means of the global chain flexibility. As confirmed by SEC-ESI MS, signals arising from bimolecular coupling are more abundant than signals arising from propagation. A propagation mechanism always involves three or more GMA units, analogous to a mechanism described for ROP (Figure 3b). As proposed, propagation forces the collapsing chain into a certain geometry, resulting from the demand of the activated glycidyl unit to react with multiple epoxides. Thus, the global chain flexibility is reduced in a short amount of time, leading to a larger loss of entropy than in a bimolecular coupling event. In more detail, we submit that the SCNP species labeled with △ at m/z 2248.1500 (exp) (2248.1492 (theor)) was formed by first reacting in a bimolecular coupling, collapsing with a maximum amount of global chain flexibility, and subsequently the residual glycidyl moieties intrachain cross-linked via propagation. The corresponding precursor p(MMA-*stat*-GMA) (**1**), with 34 units of MMA and 5 units of GMA, was assigned as a peak at m/z 2251.6378 (exp) (2251.6189 (theor)). Based on the knowledge of the present SEC-ESI MS study and with regard to the literature, we propose the following cross-linking mechanism, taking p(MMA_{34}-*stat*-GMA_5) (**2**) as model precursor: The Lewis acid catalyst activates the epoxide; due to the high dilution, a further epoxide in close proximity ring-opens the activated one. If the highly reactive oxiranium species does not find a further reaction partner, it becomes quenched by residual water. The three remaining epoxides cross-link via propagation (forming species △) or via bimolecular coupling (forming species ∞ after the last epoxide reacts with water). Alternatively, the oxiranium ion can also react via an elimination reaction, forming a double bond adjacent to the oxygen (species ⊕). However, under high dilution, the propagating oxiranium can undergo a macrocyclization reaction as described by Barroso-Bujans and coworkers.[17b] These two termination reactions (elimination and cyclization) result in completely identical (isobaric) structures.

To investigate if the mode of catalyst addition to the reaction mixture has any fundamental influence on the folding mechanism, we performed an experiment adding $B(C_6F_5)_3$ over a period of several hours, using a syringe pump and a flow rate of 1 mL·h^{-1}. Surprisingly, the SEC trace of the prepared SCNP **2** (Figure S3) only indicates a slight shift toward higher retention volume. Comparing the mass spectra obtained by direct addition (Figure 1c) and over a period of several hours (Figure S5) gave similar mass signals. Thus, a SCNP collapse took place, but—as evidenced by the SEC trace—to a lesser degree as observed by direct addition of the Lewis acid. A comparison of both double-charged single oligomer profiles revealed an extremely broadened isotopic pattern for some of the peaks (Figure S5). Adding the catalyst over a period of several hours seems to produce preferably species resulting from a bimolecular coupling (labeled with ●). Utilizing the isotopic simulation as a sensor, we found a ratio of the species labeled with ●:△:⊡:⌀ = 10:3:4:3 in the case of direct addition of the catalyst. Instead, using the syringe pump, we were able to assign the ratio after quantitative isotopic simulation to be ●:△:⊡:⌀ = 10:1:0:0 (Figure S16). Important species being formed via propagation events (labeled with △ and ⊡) are decreased significantly. Moreover, the species labeled with ⌀ at

DOI: 10.1021/jacs.6b10952
J. Am. Chem. Soc. 2017, 139, 51−54

m/z 2250.6579 (exp) (2250.6423 (theor)) as a product of three consecutive bimolecular coupling events is absent. Consequently, the slight shift to higher retention time might be explained by strong reduction of propagation and multiple bimolecular coupling events. As mechanistically suggested, propagation forces the collapsing chain into a certain geometry, which might be more compact and thus small in its hydrodynamic radius. In contrast, bimolecular coupling allows the chain to almost keep its initial conformation. The forming loop results in only a slight conformational changes and thus in slight reduction of the hydrodynamic radius.

Finally, we explored the mass spectrometric changes by varying the GMA feed ratio from initial 15% to 10%, collapsing the chains via direct addition of the catalyst. The mass spectrum obtained of the SCNP **2** with 10% cross-links does not differ significantly from that having a GMA feed ratio of 15% (Figure S18). Still, species as a result of a bimolecular coupling (e.g., at m/z 2258) are very abundant. Broadened isotopic patterns indicate the presence of propagation and multiple bimolecular coupling events. Thus, a reduction of GMA does not favor one mechanistic pathway and thereby suppress the other one.

In summary, we introduce SEC-ESI MS as a powerful technique to assess the folding of a collapsed linear polymer into a single-chain nanoparticle. Poly(MMA-*stat*-GMA) (**1**) meets essential requirements for the successful ionization, as well as the resulting SCNP folded via ring-opening chemistry. We clearly identify two distinct pathways of SCNP collapse that can only be identified by high-resolution mass spectrometry. Specifically, besides finding bimolecular coupling to be the dominant, entropically favored cross-linking process, we were able to assign species arising from a propagation pathway. Our work constitutes a novel characterization platform for SCNPs that can be employed for all SCNP systems that ionize well and provides critical molecular information regarding the folding process.

■ ASSOCIATED CONTENT

Supporting Information

The Supporting Information is available free of charge on the ACS Publications website at DOI: 10.1021/jacs.6b10952.

Experimental details and characterization data, including Figures S1−S18 and Tables S1−S3 (PDF)

■ AUTHOR INFORMATION

Corresponding Author

*christopher.barner-kowollik@kit.edu; christopher.barnerkowollik@qut.edu.au

ORCID

Christopher Barner-Kowollik: 0000-0002-6745-0570

Notes

The authors declare no competing financial interest.

■ ACKNOWLEDGMENTS

C.B.-K. acknowledges the Sonderforschungsbereich 1176 (project A2) funded by the German Research Council (DFG) as well as continued funding from the Karlsruhe Institute of Technology and the Helmholtz association via the BioInterfaces in Technology and Medicine and the Science and Technology of Nanosystems programs. Additional support from the Queensland University of Technology is acknowledged. J.S.'s studies are funded by a Landesgraduierten Scholarship of the State of Baden-Wuerttemberg.

■ REFERENCES

(1) (a) Altintas, O.; Barner-Kowollik, C. *Macromol. Rapid Commun.* **2012**, *33*, 958. (b) Altintas, O.; Barner-Kowollik, C. *Macromol. Rapid Commun.* **2016**, *37*, 29. (c) Sanchez-Sanchez, A.; Pomposo, J. A. *Part. Part. Syst. Charact.* **2014**, *31*, 11. (d) Lyon, C. K.; Prasher, A.; Hanlon, A. M.; Tuten, B. T.; Tooley, C. A.; Frank, P. G.; Berda, E. B. *Polym. Chem.* **2015**, *6*, 181. (e) Mavila, S.; Eivgi, O.; Berkovich, I.; Lemcoff, N. G. *Chem. Rev.* **2016**, *116*, 878. (f) Hanlon, A. M.; Lyon, C. K.; Berda, E. B. *Macromolecules* **2016**, *49*, 2. (g) Ouchi, M.; Badi, N.; Lutz, J.-F.; Sawamoto, M. *Nat. Chem.* **2011**, *3*, 917.

(2) Schmidt, B. V. K. J.; Fechler, N.; Falkenhagen, J.; Lutz, J.-F. *Nat. Chem.* **2011**, *3*, 234.

(3) (a) Willenbacher, J.; Altintas, O.; Trouillet, V.; Knöfel, N.; Monteiro, M. J.; Roesky, P. W.; Barner-Kowollik, C. *Polym. Chem.* **2015**, *6*, 4358. (b) Sanchez-Sanchez, A.; Arbe, A.; Colmenero, J.; Pomposo, J. A. *ACS Macro Lett.* **2014**, *3*, 439. (c) Greb, L.; Mutlu, H.; Barner-Kowollik, C.; Lehn, J. M. *J. Am. Chem. Soc.* **2016**, *138*, 1142.

(4) (a) Foster, E. J.; Berda, E. B.; Meijer, E. W. *J. Am. Chem. Soc.* **2009**, *131*, 6964. (b) Romulus, J.; Weck, M. *Macromol. Rapid Commun.* **2013**, *34*, 1518.

(5) (a) Altintas, O.; Willenbacher, J.; Wuest, K. N. R.; Oehlenschlaeger, K. K.; Krolla-Sidenstein, P.; Gliemann, H.; Barner-Kowollik, C. *Macromolecules* **2013**, *46*, 8092. (b) De Luzuriaga, A. R.; Ormategui, N.; Grande, H. J.; Odriozola, I.; Pomposo, J. A.; Loinaz, I. *Macromol. Rapid Commun.* **2008**, *29*, 1156.

(6) Tuten, B. T.; Chao, D.; Lyon, K.; Berda, E. B. *Polym. Chem.* **2012**, *3*, 3068.

(7) Niemeyer, C. M. *Angew. Chem., Int. Ed.* **2001**, *40*, 4128.

(8) Willenbacher, J.; Wuest, K. N. R.; Mueller, J. O.; Kaupp, M.; Wagenknecht, H. A.; Barner-Kowollik, C. *ACS Macro Lett.* **2014**, *3*, 574.

(9) Terashima, T.; Mes, T.; De Greef, T. F. A.; Gillissen, M. A. J.; Besenius, P.; Palmans, A. R. A.; Meijer, E. W. *J. Am. Chem. Soc.* **2011**, *133*, 4742.

(10) Frank, P. G.; Tuten, B. T.; Prasher, A.; Chao, D.; Berda, E. B. *Macromol. Rapid Commun.* **2014**, *35*, 249.

(11) Pomposo, J. A.; Perez-Baena, I.; Lo Verso, F.; Moreno, A. J.; Arbe, A.; Colmenero, J. *ACS Macro Lett.* **2014**, *3*, 767.

(12) Gruendling, T.; Weidner, S.; Falkenhagen, J.; Barner-Kowollik, C. *Polym. Chem.* **2010**, *1*, 599.

(13) Cecchini, M. M.; Steinkoenig, J.; Reale, S.; Barner, L.; Yuan, J.; Goldmann, A. S.; De Angelis, F.; Barner-Kowollik, C. *Chem. Sci.* **2016**, *7*, 4912.

(14) Fast, D. E.; Zalibera, M.; Lauer, A.; Eibel, A.; Schweigert, C.; Kelterer, A.-M.; Spichty, M.; Neshchadin, D.; Voll, D.; Ernst, H.; Liang, Y.; Dietliker, K.; Unterreiner, A.-N.; Barner-Kowollik, C.; Grützmacher, H.; Gescheidt, G. *Chem. Commun.* **2016**, *52*, 9917.

(15) Gruendling, T.; Hart-Smith, G.; Davis, T. P.; Stenzel, M. H.; Barner-Kowollik, C. *Macromolecules* **2008**, *41*, 1966.

(16) Perez-Baena, I.; Barroso-Bujans, F.; Gasser, U.; Arbe, A.; Moreno, A. J.; Colmenero, J.; Pomposo, J. A. *ACS Macro Lett.* **2013**, *2*, 775.

(17) (a) Britovsek, G. J. P.; Ugolotti, J.; White, A. J. P. *Organometallics* **2005**, *24*, 1685. (b) Asenjo-Sanz, I.; Veloso, A.; Miranda, J. I.; Pomposo, J. A.; Barroso-Bujans, F. *Polym. Chem.* **2014**, *5*, 6905.

(18) (a) Sunder, A.; Hanselmann, R.; Frey, H.; Mülhaupt, R. *Macromolecules* **1999**, *32*, 4240. (b) Tokar, R.; Kubisa, P.; Penczek, S.; Dworak, A. *Macromolecules* **1994**, *27*, 320.

(19) Tracy, J. B.; Kalyuzhny, G.; Crowe, M. C.; Balasubramanian, R.; Choi, J.; Murray, R. W. *J. Am. Chem. Soc.* **2007**, *129*, 6706.

(20) Gruendling, T.; Guilhaus, M.; Barner-Kowollik, C. *Anal. Chem.* **2008**, *80*, 6915.

(21) Konermann, L.; Ahadi, E.; Rodriguez, A. D.; Vahidi, S. *Anal. Chem.* **2013**, *85*, 2.

(22) Pahnke, K.; Brandt, J.; Gryn'ova, G.; Lindner, P.; Schweins, R.; Schmidt, F. G.; Lederer, A.; Coote, M. L.; Barner-Kowollik, C. *Chem. Sci.* **2015**, *6*, 1061.

DOI: 10.1021/jacs.6b10952
J. Am. Chem. Soc. 2017, 139, 51−54